Oxide-Assisted Catalytic Growth of MgO Nanowires with Uniform Diameter Distribution

Chengchun Tang,* Yoshio Bando,* and Tadao Sato

Advanced Materials Laboratory, National Institute for Materials Science, 1-1 Namiki, Tsukuba, Ibaraki 305-0044, Japan

Received: March 22, 2002; In Final Form: May 16, 2002

MgO nanowires with uniform diameter distribution of about 20 nm have been synthesized by boron oxide-assisted catalytic growth method. X-ray diffraction, scanning electron microscopy, and high-resolution transmission electron microscopy were used to characterize the structure and defects. The results indicate that MgO nanowires are single-crystal face-centered cubic structures with the growth axis of [100] for straight nanowires. The bending of MgO nanowires could also be observed and explained based on the switching of growth direction from [100] to [201] and to [301]. The contamination from the reactant boron oxide results in the rectangular domain defects. The growth mechanism was also proposed for the synthesis of MgO nanowires.

1. Introduction

There has been much interest in one-dimensional nanoscale materials due to their potential in mesoscopic physics and nanodevice technique.[1−3] A variety of one-dimensional nanostructure with different morphologies and compositions, such as carbon nanotubes[4] and semiconductor nanowires (and nanotubes) comprised by nitride,[5] carbide,[6] phospide,[7] sulfide[8] and element,[9,10] have been successfully fabricated by various techniques including carbon nanotube confined reaction, arc discharge, laser ablation, physical evaporation, and chemical vapor deposition. Recently, much attention has been paid to oxide one-dimensional nanostructures due to their interesting properties and applications in optics, magnetism, superconductivity, and ferroelectricity. A series of binary oxide nanobelts including ZnO,[11] CdO,[12] In_2O_3,[11] PbO_2,[13] SnO_2,[14] and Ga_2O_3[12] have been synthesized by simple physical evaporation. Other techniques, such as vapor-solid process and catalytic growth, have also been used to synthesize GeO_2,[15] MgO,[16] Al_2O_3,[17] Ga_2O_3,[18] and In_2O_3[19] nanowires (nanorods).

Among the mentioned synthesis methods, catalytic growth is particularly suitable for the growth of nanowires with uniform diameter distribution on a large scale because it provides an additional diameter control of nanowires by the dimension of catalytic nanoparticles. In fact, catalytic growth originates from the conventional vapor−liquid−solid growth mechanism.[20] Therein, an impurity provides a pathway of a continuously growing wire-like structure and therefore can be considered as catalyst. The reactant vapors are absorbed into the liquid-phase catalyst and crystallized in a solid-phase wire-like product via a eutectic growth process. Within the framework of catalytic growth, the synthesis of nanowires depends mainly on the following three factors: the formation of nanoscale liquid-phase catalyst, the continuous supply of reactant vapors, and the existence of a eutectic reaction area in the corresponding phase diagram.

Recently, we reported an improvement of the procedure to synthesize oxide and nitride nanowires,[17,18] along with boron nitride nanotubes,[21] by using a silica-assisted catalytic growth method. The addition of silica reduces the wetting temperature of transition metal catalyst, and in-situ provides reaction vapor enough to continuously synthesize nanowires. However, owing to the high reaction barrier potential between silica and metal, the catalytic formation of nanowires needs a high reaction temperature. A high reaction temperature might result in the agglomeration of catalytic particles and consequently increase the nanowires' diameters or modify their morphologies, probably destroying their catalytic activity. Another significant disadvantage of the silica-assisted catalytic growth method is that it would be hard to separate the synthesized nanowires from silica solid grain.

Here we report a vitreous boron oxide-assisted catalytic growth method by demonstrating the synthesis of MgO nanowires with uniform diameter distribution. In comparison with the silica-assisted method, the vitreous boron oxide-assisted growth procedure is particularly suitable for the low-temperature nanowires growth from volatile metals and it is easy to remove the boron oxide impurity from the final product by simply washing with chemical solvents.

2. Experimental Methods

Fe_2O_3 catalysts were prepared using the same method as that used in catalytic growth of GaN nanowires described previously.[22] Fumed alumina was stirred with methanol, and the resulting slurry was put inside a methanol solution of ferric nitrate. The combined slurry was stirred for several hours, dried in a rotary evaporator, and baked in vacuum at 150 °C overnight followed by grinding into a fine powder. The diameter of the transition metal oxide nanoparticle ranges from 15 to 25 nm.

A 1 g portion of the as-prepared catalysts was thoroughly mixed with 3 g of boron oxide powder by ball-milling for 6 h. A 1 g portion of metal magnesium was placed in an alumina crucible and then was covered by 4 g of the as-prepared mixture. The crucible was placed into a sintered alumina tube held in a conventional furnace. Argon was flowing at a rate of 80 sccm during the overall reaction period as a transport and protective gas. The furnace was first heated to reach 500 °C in 10 min and was kept for another 10 min to make vitreous boron oxide,

* Corresponding authors. E-mail: Tang.chengchun@nims.go.jp. E-mail: Bando.Yoshio@nims.go.jp.

10.1021/jp0207883 CCC: $22.00
Published on Web 07/09/2002

which forms an extremely viscous layer to cover the metal magnesium and preclude its evaporation at a high rate. Subsequently, the furnace was again heated to reach 850 °C in 20 min. The reaction lasted for 1 h before the furnace was cooled to room temperature. After reaction, a colorless sponge-like product was found to cover the surface of a black glassy crust and can be easily collected. The black glassy crust is located at the area of the starting boron oxide and catalyst. The reaction magnesium metal was fully evaporated. Some colorless powder was also collected from the inner wall of alumina crucible and tube.

Our further experiments indicated that the occurrence of the colorless sponge-like product is insensitive to the flow rates of the protective argon gas and the reaction temperature from 800 to 850; however, the maximum yield could be obtained when the experimental procedure described above is adopted. When the excess metal magnesium, the weight ratio between B_2O_3 and catalysts lower than 2:1 or the short duration time at 500 °C making vitreous B_2O_3, was used, only less sponge-like product could be obtained. This indicated that the effectively covered vitreous boron oxide layer is the key to obtaining sponge-like product.

The crystal structure and phase purity of the products were examined by means of X-ray diffraction (XRD) analysis with Cu Kα radiation. The overview of the sample morphology was checked by scanning electron microscopy (SEM). Sample powders were ultrasonically dispersed in acetone and dropped onto a carbon-coated copper grid for transmission electron microscopy (TEM). High-resolution TEM was carried out by a field emission electron microscope (JEM-3000F, JEOL) operating at 300 kV. Energy-dispersive X-ray analysis (EDS) and electron energy-loss spectra (EELS) were employed for identifying the elemental compositions of the products.

3. Results

XRD measurement indicates that the black glassy crust mainly consists of boron oxide and little magnesium borate, and the colorless powder collected from the inner wall of tube and crucible dominantly exhibits face-centered cubic MgO structure with B_2O_3 and Mg. SEM examinations indicate that no one-dimensional morphologies could be observed from the colorless powders. However, the one-dimensional structure can be well established from the sponge-like product collected from the surface of the glassy crust.

Figure 1 shows the XRD pattern of the sponge-like product. Except for the peaks with weak intensity that are labeled in star in the figure and are assigned to hexagonal B_2O_3 (JCPDS 73-2100), the pattern can be appropriately indexed in peak position as a face-centered cubic structure of MgO with lattice parameter of $a = 0.429$ nm, which is consistent with the calculated value of 0.42123 nm (JCPDS 78-0430). However, the peak intensities exhibit considerably differently between the present XRD pattern and the calculated pattern. The ideal intensity ratio between (220) and (200) is about 0.5, whereas the measured ratio in this study is smaller than 0.2. The intensity from the (220) diffraction is strongly depressed. This phenomenon has also been observed for GaP nanorods[7] and Al_2O_3 whiskers[23] and was attributed to preferential growth of wire structure. As a result, the present MgO crystal should grow along the [100] axis and perpendicular to the (220) plane.

Figure 2 shows the typical SEM image of the sponge-like sample, indicating that the product is slightly curved nanowires with the uniform diameter of about 20 nm and the typical length of several tens of micrometers. However, several hundred

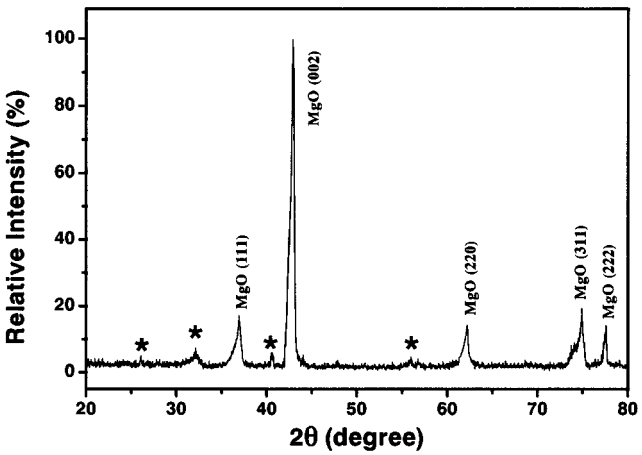

Figure 1. XRD pattern of MgO nanowires collected from the surface of the glassy crust. The reflections of MgO crystal are marked by their indices. The unindexed starred peaks are assigned to hexagonal boron oxide.

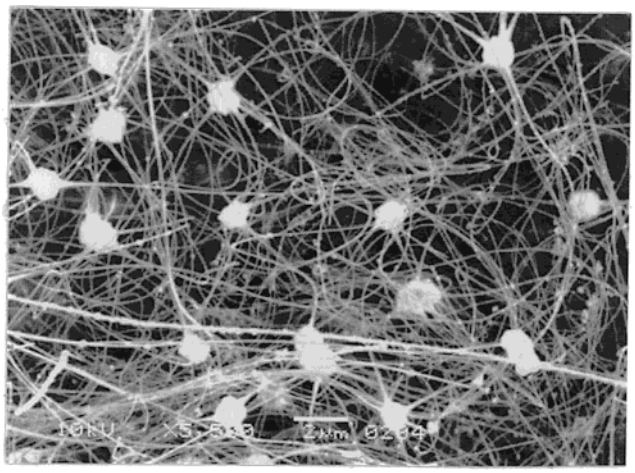

Figure 2. SEM image of MgO nanowires. MgO nanowires grow from a sphere-like particle with micrometer scale to form nanoflower morphology. Curved and ring-like MgO nanowires also exist in the sample. A great amount of boron oxide particle were found to attach to the surface of MgO nanowires, as observed for the MgO nanowires with relatively large diameter distribution and with relatively bright contrast.

micrometer nanowires can also be observed frequently in SEM images. Some ring-like nanowires could be clearly found. SEM images also reveal that all of the MgO nanowires grow radiantly from the sphere-like particles and therefore exhibit the so-called nanoflower morphology, which has been reported for the silicon-based one-dimensional nanostructure.[24] We noticed that these nanoparticles usually have the size of about 1 micrometer and most of the nanowires grow symmetrically from the particles. EDS measurements for the nanoparticles show the presence of MgO and B_2O_3, in addition to Al_2O_3 and Fe_2O_3 of the starting catalysts as minor constituents, while the nanowires only consist of Mg and O. This indicates that the formation of MgO nanowires is based on the catalytic growth mechanism and B_2O_3 plays an important role in forming liquid-phase catalyst. Except being in catalytic particles, B_2O_3 particles with nanoscale size also are observed to attach to the outer surface of MgO nanowires, as shown in Figure 2.

The nanoparticles containing B_2O_3 could be easily removed when preparing TEM specimen using an ultrasonic dispersion method. TEM observations indicate that only little B_2O_3 with strongly chemical interaction to MgO could attach to nanowires

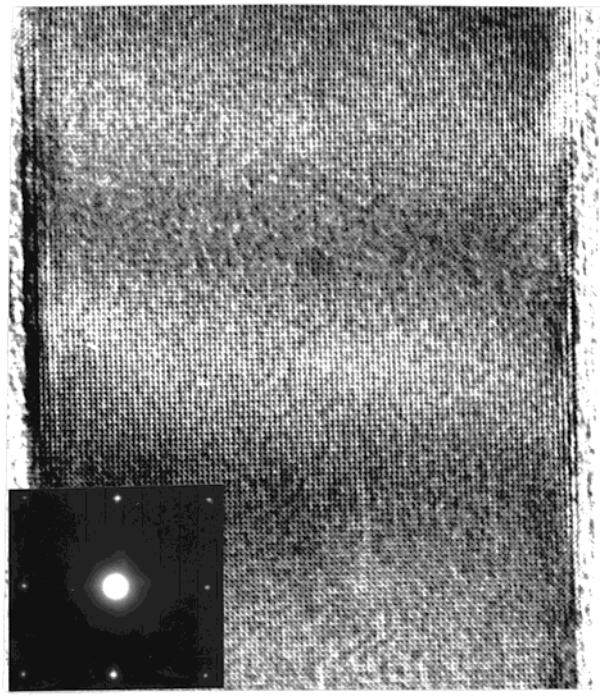

Figure 3. High-resolution TEM image of MgO nanowire. The growth direction is along [100]. The corresponding selected area electron diffraction pattern is also shown in the inset.

and consequently modify the surface morphology of MgO nanowires (see below). Figure 3 shows a typical high-resolution TEM image of an MgO nanowire with smooth surface and no B_2O_3 attachment. The nanowire is about 23 nm in diameter and exhibits considerably planar defects including twin crystals and stacking faults. The measurable planar distance is 0.21 nm, corresponding to the spacing of {002}. The selected area electron diffraction recorded with the electron beam perpendicular to the axis of the MgO nanowire is also shown in Figure 3, indicating the single-crystal nature of MgO nanowires. Combining high-resolution TEM and defocus electron diffraction technique, the axis direction of MgO nanowires could be determined as [100] growth, which is in agreement with the deduction from the XRD analysis.

The existence of planar defects is responsible for the bending of MgO nanowires observed from the SEM image shown in Figure 2. A typical TEM image exhibiting the bending is shown in Figure 4. The most commonly observed bending angles are 90°, 26°, and 18°. This is the result of switching the growth direction from [100] to [010], [201], and [301] direction, respectively. Some continuous changes of growth direction from [100] to [201] and to [301] and so on could also be observed for an individual MgO nanowire. We believe that the occurrence of ring-like MgO nanowires observed from the SEM image shown in Figure 2 results from this continuous bending. Except for the bending of individual nanowires, some MgO nanowires are found to grow from another nanowire surface and thus form a branchy structure. Only 90° growth branch could be observed from TEM images, and no catalyst particles could be detected from the cross point between two MgO nanowires, indicating that the growth of branchy structure originates from the same planar defect mechanism of the switching of growth direction with 90° angle.

Although the reactant B_2O_3 remnant in the product could be easily removed, the chemical interaction between B_2O_3 and MgO crystal could be frequently observed from TEM images. The interaction might take place in the process of synthesizing

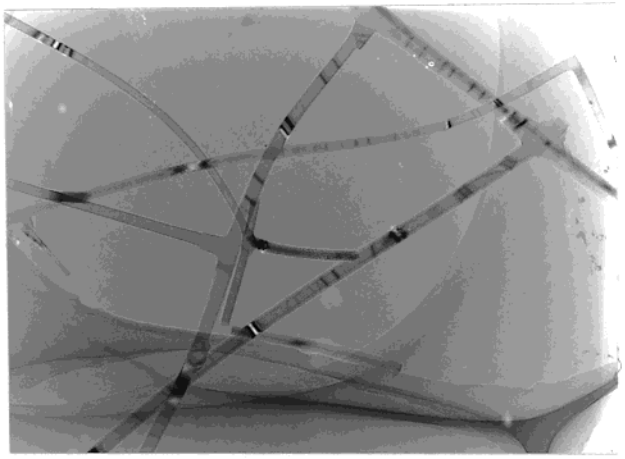

Figure 4. TEM image of MgO nanowires with curved and branchy morphologies.

MgO nanowires or be due to the radiation of electron beam under TEM examination. Figure 5a shows a typical morphology of MgO nanowires with B_2O_3 contamination. A great amount of relatively bright contrasts could be easily observed from the surface of the straight MgO nanowires grown along the [100] axis. Figure 5b gives the corresponding high-resolution TEM image. It can be seen that there are many rectangular domain defects with orientation parallel to the [100] axis. Therefore, the orientation relationship of the surface of MgO nanowire should be disordered distribution of {200}. The domain defects could be easily observed from the corresponding electron diffraction, as shown in Figure 5c. EELS and EDS measurements by means of a nanobeam technique for the domain defects indicate that boron exists at the domain area, while the areas without domain structures do not contain boron. An EDS spectrum from the domain area is shown in Figure 5d.

4. Discussion

The oxidation of magnesium in the absence of catalyst results in irregular particle-like structures, which are observed from the products collected from the inner wall of reaction tube and crucible. Therefore, the growth of the present MgO nanowires should be involved in the oxide-assistant catalytic growth mechanism. Compared with the silica-assisted method, the vitreous boron oxide-assisted method is particularly suitable for the low-temperature growth from volatile metals within the framework of the catalytic growth mechanism. First, the chemistry of boron oxide is dominated by the Lewis acid character of the BO_3 unit, and it is usually used as high-temperature flux due to its melting point of about 450 °C and the high viscosity of the molten form.[25] The mixture of boron oxide and supported catalysts forms a dense vitreous layer to cover the volatile magnesium metal and preclude it from evaporating at a high rate. This ensures a relatively slow transport rate and a stable concentration of reacted gas to exist near to the transition metal oxide catalysts. Second, catalytic growth needs to provide a liquid-phase impurity as solvent to absorb reactant vapors. Usually, transition metals or their oxides possess a high melting point, and it is higher than 1500 °C for bulk iron or its oxide. Although the melting point of nanoscale iron oxide might be lower than the corresponding bulk material,[26] the reaction temperature of 850 °C is still not high enough to melt iron. However, it has been reported that molten boron oxide has strongly solvent and fluxing action to iron- or cobalt-based compounds,[25] the chemical actions result in the formation

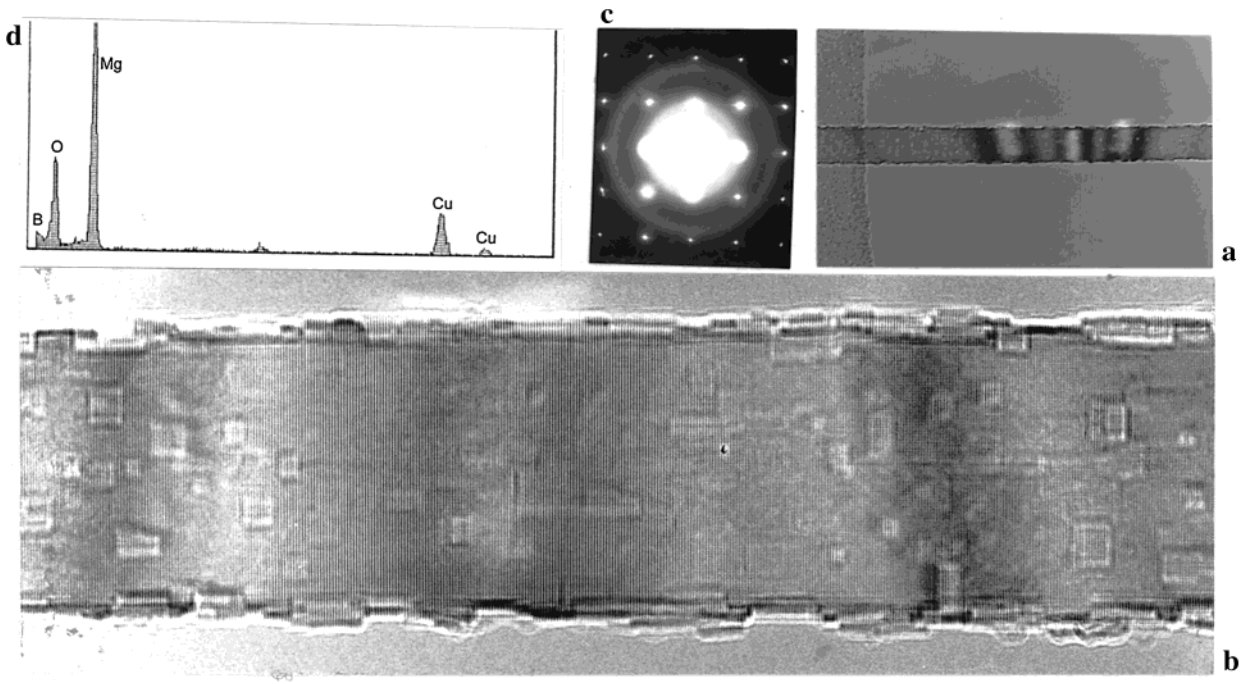

Figure 5. MgO nanowire with boron oxide contamination: (a) low-magnification TEM image; (b) high-resolution TEM image, some rectangular domain defects could be easily observed; (c) selected-area electron diffraction pattern; (d) EDS spectrum from the domain area.

of an Fe−B−O mixed phase and wet the supported iron oxide catalyst. Third, it is also likely that the catalysts tend to form larger spherical particles due to the boron oxide flux action mentioned above. Therefore, the catalytic aggregations are in an unstable condition. When the metal vapors are absorbed by the catalytic aggregation, a complicated Fe−B−Mg−O droplet is thus formed. At the reaction temperature of 850 °C, magnesium reacts with boron oxide inside the liquid-phase catalysts to nucleate MgO crystal and begin wire-like growth when the MgO becomes saturated. Owing to being in an unstable state, the catalytic aggregation will vary its size or shape when solid nanorods grow from the droplet. Therefore, it is easy to form the different catalytic nucleation points and to begin the growth of another MgO nanowire. This assumption could be used to explain the nanoflower-like growth.

In addition, the alumina supported iron oxide particles with uniform diameter of about 20 nm are responsible for the synthesis of MgO nanowires with similar diameter distribution. The support alumina could effectively preclude the iron oxide particles from agglomerating, and the size of catalyst particles thus could be preserved at the present reaction temperature. It is commonly accepted knowledge that the size of the used catalysts plays an important role in determining the diameter and formation of nanowires. Therefore, MgO nanowires synthesized here have a uniform diameter distribution.

5. Summary

In this study, we have demonstrated the synthesis of cubic MgO nanowires with uniform diameter of about 20 nm by a modified oxide-assisted catalytic growth method. Alumina supported iron oxide nanoparticles were used as catalysts to control the diameter of the synthesized MgO nanowires, and boron oxide was used as the assisted oxide to wet the catalyst and provide an oxygen source. In comparison to the previously reported silica-assisted growth method, the boron oxide-assisted catalytic growth is particularly suitable for the synthesis of metal oxide nanowires by evaporating volatile metals. We believe that the proposed synthesis mechanism should be used to synthesize other nanowires including ZnO, CdO, In_2O_3, and Al_2O_3 at low reaction temperatures.

References and Notes

(1) Alivisatos, A. P. *Science* **1996**, *271*, 933.
(2) Duan, X.; Huang, Y.; Cui, Y.; Wang, J.; Lieber, C. M. *Nature* **2001**, *409*, 66.
(3) de Heer, W. A.; Chatelain, A.; Ugate, D. *Science* **1995**, *270*, 1179.
(4) Iijima, S. *Nature* **1991**, *354*, 56.
(5) Han, W.; Fan, S.; Li, Q.; Hu, Y. *Science* **1997**, *277*, 1287.
(6) Dai, H.; Wong, E. W.; Lu, Y. Z.; Fan, S.; Lieber, C. M. *Nature* **1995**, *375*, 769.
(7) Tang, C.; Fan, S.; de la Chapelle, M. L.; Dang, H.; Li, P. *Adv. Mater.* **2000**, *12*, 1346.
(8) Tenne, R.; Margulis, L.; Genut, M.; Hodes, G. *Nature* **1992**, *360*, 444.
(9) Morales, A. M.; Lieber, C. M. *Science* **1998**, *279*, 208.
(10) Lee, S. T.; Wang, N.; Zhang, Y. F.; Tang, Y. H. *Mater. Res. Bull.* **1999**, *24*, 36.
(11) Pan, Z. W.; Dai, Z. R.; Wang, Z. L. *Science* **2001**, *291*, 1947.
(12) Dai, Z. R.; Pan, Z. W.; Wang, Z. L. *Solid State Commun.* **2001**, *118*, 351.
(13) Pan, Z. W.; Dai, Z. R.; Wang, Z. L. *Appl. Phys. Lett.* **2002**, *80*, 309.
(14) Dai, Z. R.; Gole, J. L.; Stout, J. D.; Wang, Z. L. *J. Phys. Chem. B* **2002**, *106*, 1274.
(15) Bai, Z. G.; Yu, D. P.; Zhang, H. Z.; Ding, Y.; Gai, X. Z.; Huang, H. L.; Xiong, G. C.; Feng, S. Q. *Chem. Phys. Lett.* **1999**, *303*, 311.
(16) Yang, P. D.; Lieber, C. M. *J. Mater. Res.* **1997**, *12*, 2981.
(17) Tang, C.; Fan, S.; Li, P.; de la Chapelle, M. L.; Dang, H. *J. Cryst. Growth* **2001**, *224*, 117.
(18) Tang, C.; Fan, S.; de la Chapelle, M. L.; Li, P. *Chem. Phys. Lett.* **2001**, *333*, 12.
(19) Liang, C.; Meng, G.; Lei, Y.; Phillipp, F.; Zhang, L. *Adv. Mater.* **2001**, 13, 1330.
(20) Wagner, R. S.; Ellis, W. C. *Appl. Phys. Lett.* **1964**, *4*, 8.
(21) Tang, C.; de la Chapell, M. L.; Fan, S.; Li, P.; Liu, Y. M.; Dang, H. Y. *Chem. Phys. Lett.* **2001**, *342*, 492.
(22) Tang, C.; Fan, S.; Dang, H.; Li, P.; Liu, Y. *Appl. Phys. Lett.* **2000**, *77*, 1961.
(23) Valcareel, V.; Souto, A.; Guitian, F. *Adv. Mater.* **1998**, *10*, 138.
(24) Zhu, Y.; Hu, W.; Hsu, W.; Terrones, M.; Grobert, N.; Karali, T.; Terrones, H.; Hare, J. P.; Townsend, P. D.; Kroto, H. W.; Walton, R. M. *Adv. Mater.* **1999**, *11*, 844.
(25) Adams, R. M. Boron, *Metallo-boron Compounds and Boranes*; Interscience Publisher: New York, 1964; p 60.
(26) Goldstein, A. N.; Echer, C. M.; Alivisatos, A. P. *Science* **1992**, *256*, 1425.